

DOE/ER/40762-253
UMD-PP#02-044

QCD evolution equations

A.V. Belitsky

*Department of Physics
University of Maryland at College Park
College Park, MD 20742-4111, USA*

Abstract

We discuss QCD evolution equations for two and three particle correlation functions of quarks and gluon fields in a hadron which describe development of the momentum distribution of a parton system with a change of the wave length of a probe which resolves it. We show in a general case of two-particle correlators how the four-dimensional conformal algebra and the known pattern of conformal symmetry breaking in QCD can be used to solve the complicated mixing problem of local operators under renormalization and compute economically anomalous dimensions of quark and gluon composite operators. An extension of QCD to $\mathcal{N} = 1$ super Yang-Mills theory and use of superconformal anomalies arising after quantization allows to derive non-trivial relations between the anomalous dimensions. For three-parton systems the conformal symmetry alone is not enough to solve the three-particle problem. We show that in multicolor limit of QCD there arises an extra conserved charge describing the solitonic motion of the system of particles. The problem admits a one-to-one correspondence with certain spin chain models which are exactly solvable.

*Talk given at the
Workshop on The Phenomenology of Large N_c QCD
Tempe, Arizona, January 9-11, 2002*

QCD EVOLUTION EQUATIONS

A.V. BELITSKY

*Department of Physics
University of Maryland at College Park
College Park, MD 20742-4111, USA*

We discuss QCD evolution equations for two and three particle correlation functions of quarks and gluon fields in a hadron which describe development of the momentum distribution of a parton system with a change of the wave length of a probe which resolves it. We demonstrate how broken space-time and hidden QCD symmetries serve to understand the structure and ultimately solve these equations.

1 Unraveling layers of matter: from atoms to partons

A wisdom goes back to ancient Greeks who philosophized that the matter consists of tiny particles — atoms. However, the atomic structure remained a puzzle till the beginning of the 20th century when the radioactivity was discovered and used by Rutherford in his seminal experiments on large angle scattering of α particles off atoms which suggested that the atom bears a localized core — the nucleus. On the other hand, electron beams were found to pass through atoms with no or very little deflection forcing Lenard to hypothesize that atoms have wide empty spaces inside. α particles having much larger wave length comparable to the nucleus size scattered more frequently with a low intensity beams than their ‘cousins’ β particles having much smaller wave length and which, for available luminosity, had a very low cross section. Similar experiments but rather with light sources or neutrons are exploited nowadays to study the crystal structure. If one puts a crystal in front of a source of visible light, the object just leaves a shadow on a screen behind it and one does not see elementary building blocks which form it. Obviously, the visible light, having the wave length $\lambda_{\text{light}} \sim 0.4 - 0.7 \mu\text{m}$ cannot do the job and resolve the internal structure of a crystal. The size of an individual atom, say hydrogen, is of order $r_{\text{atom}} \sim (\alpha_{\text{em}} m_e)^{-1} \sim (10 \text{ KeV})^{-1}$. Therefore, to ‘see’ atoms in crystals one has to have photons with a comparable or smaller wave length $\lambda_\gamma \leq r_{\text{atom}}$, or equivalently, of energy $E_\gamma \geq r_{\text{atom}}^{-1}$. To do this kind of ‘nano-photography’ one need a beam of X-rays. To go beyond and look into the structure of atoms one needs even smaller wave lengths.

After the discovery of nucleus’ building blocks — nucleons, i.e., protons and neutrons, the attention has been shifted to the study of these ‘elementary’ particles. However, their elementarity has been questioned starting from

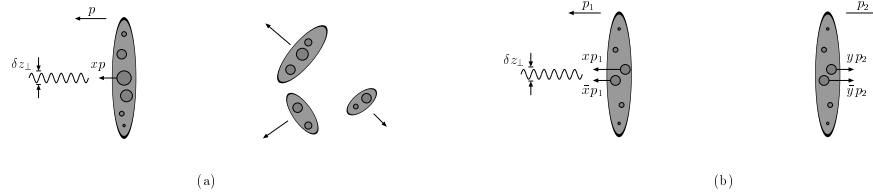


Figure 1. Partonic picture of inclusive (a) and exclusive (b) scattering of a γ^* -probe from the nucleon.

Stern's measurements in 1933 that demonstrated a large proton's magnetic moment. Hofstadter's experiments with elastic electron scattering off nucleons, $eN \rightarrow e'N'$, and measurement of their charge distribution revealed that the nucleon has a spatial extent of order 1 fm. To probe femtometer scales one has resort to scattering experiments with high energy beams. Inelastic lepton-nucleon scattering experiments, $eN \rightarrow e'X$, conducted at SLAC fulfilled this goal and led finally to the discovery of a new layer of matter by observing events with the transfer of a large momentum from the electron to the proton. If the latter would be a hard ball or a diffuse distribution of matter, such kind of scattering would be improbable. Rather it was explained by conjecturing the existence of point-like constituents inside the nucleon which absorb a highly virtual γ^* -quantum emitted by leptons, see Fig. 1 (a). Analogous representations holds for the elastic scattering alluded to above, Fig. 1 (b). These partons are nothing else than QCD quark and gluons described by a rigid $SU(3)$ gauge field theory.

2 Hard scattering and QCD

A QCD scattering amplitude is given by a successive sequence of interactions and free propagations through rife intermediate states created by QCD field operators. At n th order in the coupling $g = \sqrt{4\pi\alpha_s}$ it reads in the time-ordered form

$$\int_{-\infty}^{\infty} dt_n \int_{-\infty}^{t_n} dt_{n-1} \dots \int_{-\infty}^{t_2} dt_1 G_{n,n-1}(t_n) V_{n-1} G_{n-1,n-2}(t_{n-1}) \dots V_1 G_{1,0}(t_1).$$

The summation in repeated indices runs over states which are eigenfunctions of free equations of motion. $V_{n,m} = \langle n|V|m \rangle$ is a matrix element of a perturbation, — the interaction potential, — and the free particle propagation is

expressed in terms of a time-underintegrated free action, S , which defines a Hamiltonian of the noninteracting system,

$$G_{n,m}(t) = \exp \{it (S_n - S_m)\} .$$

At this point, one immediately concludes that there is no sensitivity to long-time scales as long as the total phase, the free particle action is time dependent ¹. In this case, cancellations of long-time contributions occur due to oscillatory nature of the integrand. However, if the phase is stationary, which corresponds to a stationary classical action, particles travel along their classical trajectories and the amplitude becomes sensitive to large-time dynamics. Since at large space-time scales α_s is large, one cannot evaluate the amplitude in a perturbative expansion and effects of quark confinement are relevant. In the opposite situation, which goes under the name of infrared safe, an observable can be computed as a power series in QCD coupling alone. These include the total inclusive σ_{tot} and jet σ_{jet} cross sections in electron-positron annihilation, etc. Indeed in $\sigma_{\text{tot}} \sim \langle 0|T\{j_\mu^\dagger j_\mu\}|0\rangle$, once a pair of quark and antiquark is created by the source j_μ , they travel back-to-back with a speed of light and cannot reassemble back into a physical state absorbed by j_μ^\dagger . Since there are no classical trajectories which allow this processes, the observable is not sensitive to infrared physics according to the criterion spelled out above.

A hard scattering cross section having at least one hadron in the initial state cannot be infrared safe since in a preparation of the asymptotic hadron state partons which form it had interacted strongly with each other for a long time in a bound state. Obviously, the wave functions of quarks in a bound state differ from what one would have if they were free. So this inevitably affects the cross section. Let us discuss in detail the deeply inelastic scattering example in Fig. 1 (a). The incoming lepton fluctuates into a lepton and a photon, $e \rightarrow e'\gamma^*$, and the latter interacts with partons in the target $|N\rangle$ fragmenting into a number of hadrons in the final state $|n\rangle$. Since the electromagnetism is very weak as compared to the strong interaction, one can restrict the analysis to a single-photon exchange with spacelike momentum q , $q^2 \equiv -Q^2$. In order to initiate a hard scattering, the electron has to pass close to one of the partons, i.e., at the distance $z^2 \sim 1/Q^2$, to exchange a photon of virtuality Q^2 . This process is described by the amplitude $\langle n|j_\mu|N\rangle$ with the local quark electromagnetic current j_μ . The measurement is totally inclusive with respect to final states and only the scattered lepton is detected. The cross section reads

$$\sigma(x_B, Q^2) = \frac{1}{\pi} \Im i \int d^4z e^{iq \cdot z} \langle N(p) | T \{ j_\mu^\dagger(z) j_\mu(0) \} | N(p) \rangle . \quad (1)$$

Let us turn to the physical picture of the deep-inelastic event in the photon-hadron center-of-mass frame. For a highly virtual photon, the transverse distance probed by it, in a Lorentz contracted hadron, is of order $\delta z_\perp \sim 1/Q$. Due to a Lorentz dilation, the virtual photon ‘sees’ the partons in a frozen state during the time of transiting the target. Therefore, since the number of parton which carry the bulk of the hadron momentum is small, the photon will ‘see’ mostly only one parton per collision. The probability for multiparton correlations is suppressed by the hard momentum,

$$n\text{-parton probability} \sim \left((\delta z_\perp)^2 / \Sigma_\perp \right)^n \sim 1 / (Q^2 \Sigma_\perp)^n, \quad (2)$$

where $\Sigma_\perp = \pi R_N^2$ is the transverse area of the nucleon of the radius R_N . These power suppressed multiparticle correlations go under the name of higher twists. Thus, to leading approximation one can restrict considerations to a single-parton scattering at high Q^2 . As compared to the inclusive annihilation mentioned above, the underlying physical picture for the forward Compton scattering admits a classical trajectory. A quark taken from the hadron absorbs the virtual photon and, as a result, accelerates. Then it reemits a photon and falls in the same momentum state. After the energy is freed into the final state the parton merges back into the parent hadron. As we already discussed above, the process is not infrared safe and depends on the quark binding inside the nucleon. The higher is the virtuality of the virtual photon Q^2 , the shorter are the distances traveled by the parton. The points of absorption and emission are separated by a light-like distance. The character of relevant distances in the Compton amplitude is a consequence of deep Euclidean kinematics $Q^2 \rightarrow \infty$. Large Q^2 and energies $\nu \equiv p \cdot q$, at fixed $x_B = Q^2/(2\nu)$, probe short distance and time structures of the process, respectively. To identify scales involved in deeply inelastic scattering let us go to a reference frame where the target proton is at rest and the virtual photon’s three-momentum is directed along the z -axis, $q = (q^0, 0, 0, q^3)$. Then

$$q = \left(\frac{Q^2}{2Mx_B}, 0, 0, \frac{Q^2}{2Mx_B} \sqrt{1 + 4M^2 x_B^2 / Q^2} \right). \quad (3)$$

For light-cone components of the momentum transfer, $q_\pm \equiv (q_0 \pm q_3)/\sqrt{2}$, we have for a large momentum transfer Q^2

$$q_- \sim Q^2 / (Mx_B), \quad q_+ \sim Mx_B. \quad (4)$$

The integrand in Eq. (1) is an oscillatory function and thus gives vanishing result unless the distances involved are

$$z_- \sim 1 / (Mx_B), \quad z_+ \sim Mx_B / Q^2. \quad (5)$$

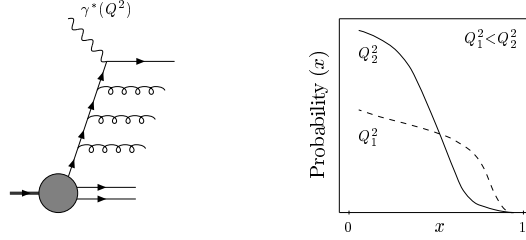


Figure 2. QCD amplitude for deeply inelastic scattering from a quark in the nucleon and resulting scaling violation (evolution) of the probability to find a parton the with a given momentum fraction x of the parent hadron with a change of the virtuality of γ^* .

Therefore, provided transverse separations z_\perp are small, the deeply inelastic scattering probes strong interaction dynamics close to the light-cone $z^2 \approx 0$, and we can neglect the dependence on all coordinate components except for z_- . The latter is called Ioffe time and has the meaning of the longitudinal distance probed in the process. Its Fourier conjugated variable is the momentum fraction x of the nucleon carried by a parton interacting with the probe. In lowest order approximation $x = x_B$.

A struck quark can emit a gluon or many gluons before actual interaction with the photon, see the left drawing in Fig. 2. When it spills a gluon the scattered quark loses a portion of its original momentum. Although it can be small for a single event, quarks tend to emit more being a relativistically moving particle. Thus, the bremsstrahlung of many gluons drifts the quark into the low momentum fraction region. Since gluons in turn can decay into a quark-antiquark pair, there is a proliferation of partons with small momentum fractions and correspondingly a decrease in the large- x domain. Thus, the probability to find a quark with small momentum fraction is higher at larger Q^2 , see the right drawing in Fig. 2. The same phenomenon can be viewed from the resolution perspective discussed above. The higher Q^2 the smaller is the distance probed by the photon. Therefore, one sees more and more partons in the cloud forming the parent ‘fat’ quark.

Since the hard subprocess occupies a very small space-time volume, the scales involved in the formation of their nonperturbative wave function are much larger, of order of a typical hadronic scale, 1 GeV. Hence, it is quite likely that they are uncorrelated and will not interfere. Thus, although the process depends on the hadronic state the parton has come from, this is basically irrelevant for the hard interactions occurred. Moreover, all final state interactions cancel in the deeply inelastic process. This is exhibited by the

relation (1) stemming from the optical theorem. Thus, there is no sensitivity to soft final-state interactions. The quantum mechanical incoherence property of physics at different scales results into the factorization property of the cross section (1). This is the base for the predictive power of perturbative QCD in many hadronic processes which one writes as

$$\sigma(x_B, Q^2) = \int dx C(x_B/x; Q^2/\mu^2) F(x; \mu^2), \quad (6)$$

where F is a parton distribution, — the probability to find a parton in the nucleon with the momentum fraction x , — and C is a perturbatively computable short-distance coefficient function.

3 Evolution equations

Due to intrinsic ultraviolet divergences, parton distributions and coefficients functions in Eq. (6) depend on a renormalization scale μ^2 . However, it cancels, as it has to, in the total result since the left-hand side being a physical observable does not depend on the arbitrary scale μ^2 . Thus, factorization implies evolution as a consequence of this independence,

$$\frac{d\sigma}{d\ln\mu^2} = 0. \quad (7)$$

Separation of variables results into complementarity equations for F and C

$$\begin{aligned} \frac{d}{d\ln\mu^2} C(x; Q^2/\mu^2) &= - \int dx' P(x/x'; \alpha_s) C(x'; Q^2/\mu^2), \\ \frac{d}{d\ln\mu^2} F(x; \mu^2) &= \int dx' P(x/x'; \alpha_s) F(x'; \mu^2). \end{aligned} \quad (8)$$

The coefficient function C is computable perturbatively and so is the evolution kernel P . The second of these equation is an inclusive evolution equation and allows to predict F at a scale μ^2 from the function F determined at some reference scale μ_0^2 . Obviously, a change in μ^2 is in one-to-one correspondence to a change in Q^2 ^a.

In the previous discussion we talked only about quark momentum probabilities. To describe a real experiment one has to account for another type of partons which are equally important dynamical degrees of freedom — gluons. Gluons contribute on equal footing with quarks and both enter in a multiplet,

^aWe will not discuss presently the evolution in longitudinal momentum with fixed transverse scales. This domain is described by another type of evolution equations addressed in ².

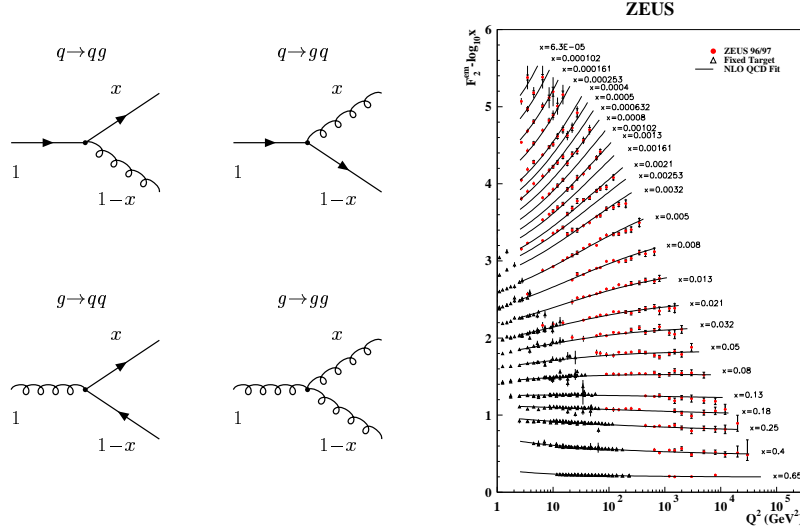


Figure 3. Elementary $a \rightarrow bc$ parton splitting amplitudes encountered at each step of the evolution (left) and a fit to experimental data ³ (right) implementing them (dressed with next-to-leading order perturbative corrections) in the evolution equation (8).

(F_q, F_g) . This multiplet obeys a matrix evolution equation of the type (8) with a quark-gluon mixing matrix of kernels

$$\mathbf{P} = \begin{pmatrix} qqP & qgP \\ gqP & ggP \end{pmatrix}, \quad \text{with} \quad {}^{ab}P(x) = |A_{a \rightarrow bc}|^2, \quad (9)$$

where $A_{a \rightarrow bc}$ represent amplitudes of elementary splittings, demonstrated in Fig. 3. The solution to the evolution equation (8), where one includes also QCD radiative corrections as well, results to a perfect description of experimental data for the unpolarized deeply inelastic cross section, shown in the same figure.

We consider below a more general case of functions which interpolates between inclusive parton distribution and exclusive distributions amplitudes and, thus, possess a very rich structure. They are known as generalized parton distributions $F(x, \eta)$ and are measurable in a number of hard exclusive reactions ^{4,5,6,7}, such as in Fig. 1 (b) with a photon emission into the final state. They admit an operator representation which reads, e.g., for quarks

$$\langle N(p_2) | \bar{q}(-z_-) q(z_-) | N(p_1) \rangle = \int dx e^{-ixz_- (p_1 + p_2)_+} F(x, \eta). \quad (10)$$

It is a correlation function of fields on the light cone separated by the distance $2z_-$ which acquire a scale dependence under renormalization. We omitted an inessential to our present consideration Dirac matrix projecting quark spinor indices. Due to different momenta of incoming and outgoing hadrons, the specifics of these functions lies in a presence of a non-zero t -channel momentum transfer $\eta = (p_2 - p_1)_+/2$, varying which one probes correlations of partons in different momentum states. The evolution equation has the same schematic form as (8),

$$\frac{d}{d \ln \mu^2} F(x, \eta; \mu^2) = \int dx' K(x/\eta, x'/\eta; \alpha_s) F(x', \eta; \mu^2). \quad (11)$$

The evolution kernel interpolates between two known limits, i.e.,

$$\lim_{\eta \rightarrow 0} K(x/\eta, x'/\eta; \alpha_s) = P(x/x'; \alpha_s), \quad \lim_{\eta \rightarrow 1} K(x/\eta, x'/\eta; \alpha_s) = V(x, x'; \alpha_s),$$

the fully inclusive case we have discussed above ($\eta = 0$) and another one which corresponds to distribution amplitudes which enter the description of a number of exclusive processes^{9,10}.

The moments of the function $F(x, \eta)$ correspond to the operator matrix elements of local operators, e.g., for quarks,

$$\int dx x^j F(x, \eta) = \langle P_2 | \bar{q} \overset{\leftrightarrow}{\partial}^j_+ q | P_1 \rangle, \quad (12)$$

where $\overset{\leftrightarrow}{\partial} \equiv \overset{\rightarrow}{\partial} - \overset{\leftarrow}{\partial}$. Under renormalization the operators in Eq. (12) get mixed with operators containing total derivatives $\partial \equiv \overset{\rightarrow}{\partial} + \overset{\leftarrow}{\partial}$ but, indeed, the same total number of derivatives as a consequence of Poincaré invariance

$$\mathcal{R}_{jk} = \bar{q} \partial_+^k \overset{\leftrightarrow}{\partial}^{j-k}_+ q. \quad (13)$$

Since the operators with total derivatives matter for each moment we have to diagonalize a $j \times j$ matrix equation,

$$\frac{d}{d \ln \mu^2} \begin{pmatrix} \mathcal{R}_{j0} \\ \vdots \\ \mathcal{R}_{jj} \end{pmatrix} = -\frac{1}{2} \begin{pmatrix} \gamma_{jj} & \cdots & \gamma_{j0} \\ & \ddots & \vdots \\ & & \gamma_{00} \end{pmatrix} \begin{pmatrix} \mathcal{R}_{j0} \\ \vdots \\ \mathcal{R}_{jj} \end{pmatrix}, \quad (14)$$

with zeros below the diagonal. The matrix has obviously a triangular form since the operator containing at least one total derivative cannot mix with operators involving none of them. Otherwise one would run in a contradiction for the forward matrix elements where total derivatives are irrelevant $\langle p | \partial(\cdots) | p \rangle = 0$. Another important observation is that the diagonal elements

of the anomalous dimension matrix are the moments of the splitting functions (9)

$${}^{ab}\gamma_j^D = -2 \int dx x^j {}^{ab}P(x). \quad (15)$$

4 Use of conformal symmetry

Recall the diagonalization of the Schrödinger equation for a hydrogen atom. The $O(3)$ symmetry of the potential allows to reduce the three-dimensional problem to a one-dimensional one, i.e., one performs a partial wave decomposition in terms of spherical harmonics. The spherical harmonics are eigenfunctions of the quadratic Casimir operator of the rotation group.

For the case at hand one can use the space-time symmetries of QCD Lagrangian to simplify significantly and ultimately solve the problem. Classical QCD is Poincaré, i.e., Lorentz $\mathcal{M}_{\mu\nu}$ and translation \mathcal{P}_μ , invariant as any realistic field theory describing nature, as well as due to absence of any dimensionful parameters for massless quarks, invariant under dilatation \mathcal{D} and special conformal \mathcal{K}_μ transformations⁸. Coordinates transform as follows under them,

$$z_\mu \xrightarrow{\mathcal{M}} \omega_{\mu\nu} z_\nu, \quad z_\mu \xrightarrow{\mathcal{P}} z_\mu + a_\mu, \quad z_\mu \xrightarrow{\mathcal{D}} \lambda z_\mu, \quad z_\mu \xrightarrow{\mathcal{K}} c_\nu (z^2 g_{\mu\nu} - z_\mu z_\nu).$$

The special conformal transformation can be visualized as a sequence $\mathcal{K}_\mu \equiv \mathcal{I}\mathcal{P}_\mu\mathcal{I}$ of inversion $\mathcal{I}z_\mu = z_\mu/z^2$, translation and inversion. This fifteen transformations form a group, $SO(4, 2)$. It is easy to construct the representation of the group on field operators using induced representations⁸. For instance, $\delta_\mu^{\mathcal{P}} q \equiv i[q, \mathcal{P}_\mu]_- = -\partial_\mu q$, etc. The eigenvectors of the quadratic Casimir operator of the projected collinear conformal group,

$$\mathbf{J}^2 = \frac{1}{2}\mathcal{P}_+\mathcal{K}_- - \frac{1}{4}(\mathcal{D} + \mathcal{M}_{-+} + 2i)(\mathcal{D} + \mathcal{M}_{-+}), \quad (16)$$

in the basis of the bilinear operators (13) are called conformal operators with eigenvalues^b

$$\mathbf{J}_{ab}^2 \mathcal{O}_{jl} = J_{ab}(J_{ab} - 1)\mathcal{O}_{jl}, \quad J_{ab} = j + j_a + j_b. \quad (17)$$

For quarks $j_q = 1$ and conformal operators are given in terms of Gegenbauer polynomials^{9,10} ($l \geq j$)

$$\mathcal{O}_{jl} = \bar{q} \partial_+^l C_j^{2j_q-1/2} \left(\partial_+^{\leftrightarrow} / \partial_+ \right) q, \quad (18)$$

^bThe indices attached to \mathbf{J}^2 stand for the conformal spin $j_a = (d_a + s_a)/2$ of fields, having the dimension d_a and spin s_a , which build \mathcal{O}_{jl} .

which is a very specific combination of local operators \mathcal{R}_{jk} (13).

Generally, the renormalization group equation reads for the conformal operators

$$\frac{d}{d \ln \mu^2} \mathcal{O}_{jl} = -\frac{1}{2} \sum_{k=0}^j (\gamma_j^D \delta_{jk} + \gamma_{jk}^{\text{ND}}) \mathcal{O}_{kl}. \quad (19)$$

As is well known a renormalization group equation is a Callan-Symanzik equation, i.e., the scale Ward identity for a Green function with a (conformal, for the case at hand) operator insertion,

$$\mathcal{G}(z_1, \dots, z_N) \equiv \int Dq D\bar{q} DA e^i \int dz \mathcal{L}(z) \mathcal{O}_{jl} \bar{q}(z_1) \dots q(z_k) \dots A(z_N). \quad (20)$$

The anomalous dimensions of operators arise due to development of an anomaly in the trace of the energy-momentum tensor,

$$\delta^D \mathcal{L} = -\Theta_{\mu\mu} = \frac{\beta_d}{g} (G_{\mu\nu}^a)^2, \quad (21)$$

where β_d is a d -dimensional QCD beta function $\beta_d = \beta + g(d-4)/2$. We did not display other terms which could not affect the physical sector¹¹. The anomalous dimensions show up in the renormalization of an operator product,

$$\mathcal{O}_{jl} i \int d^d z \Theta_{\mu\mu}(z) = \sum_{k=0}^j (\gamma_j^D \delta_{jk} + \gamma_{jk}^{\text{ND}}) \mathcal{O}_{kl}. \quad (22)$$

Since the conformal algebra is fulfilled on interacting (Heisenberg) field operators one can derive a constraint on the anomalous dimension from it. It is provided by the commutator

$$[\mathcal{D}, \mathcal{K}_\mu] = i\mathcal{K}_\mu, \quad (23)$$

which results into a commutator equation¹¹

$$\left[\gamma^D + \gamma^{\text{ND}}, a + \gamma^c + 2\frac{\beta}{g}b \right]_- = 0, \quad (24)$$

in terms of α_s -independent matrices a and b ; QCD beta-function β and a special conformal anomaly γ^c which arises, similarly to Eq. (22), in the renormalization of the product

$$\mathcal{O}_{jl} \int d^d z \delta_-^{\mathcal{K}} \mathcal{L}(z) = \sum_{k=0}^j \gamma_{jk}^c \mathcal{O}_{k,l-1}. \quad (25)$$

The special conformal variation of the action is given in terms of a coordinate moment of the energy-momentum tensor, $\delta_-^{\mathcal{K}} \mathcal{L}(z) = -2z_- \Theta_{\mu\mu}(z)$.

One can immediately draw important conclusions from Eq. (24). If one is interested in the one-loop anomalous dimension matrix, $\mathcal{O}(\alpha_s)$, one has to keep the α_s -independent term a only and write $[\gamma^{D(0)} + \gamma^{ND(0)}, a] = 0$. Since the matrix a is diagonal¹¹ we conclude that $\gamma^{ND(0)} = 0 \cdot \alpha_s$. At next-to-leading order, we have to account for β and γ^c in one-loop approximation. This provides via Eq. (24) an expression for two-loop nondiagonal elements $\gamma^{ND(1)}$ in terms of $\gamma^{D(0)}$, β_0 and $\gamma^{c(0)}$,

$$\gamma^{ND(1)} = \left[\gamma^{D(0)}, \frac{b}{a} (\beta_0 - \gamma^{D(0)}) + \frac{\gamma^{c(0)}}{a} \right]_- . \quad (26)$$

No two-loop calculation has to be done! The diagonal anomalous dimensions γ^D coincide with the anomalous dimension of local operators without total derivatives and are available in the literature on deeply inelastic scattering.

5 Use of superconformal symmetry

As we shall see momentarily, supersymmetry provides relations between the anomalous dimensions of conformal operators, while the extension to superconformal case results into identities between the special conformal anomalies γ^c of quark and gluon operators.

If one puts the QCD quarks into the adjoint representation of the color group and sets the number of flavors to one, one recovers $\mathcal{N} = 1$ super-Yang-Mills theory in the Wess-Zumino gauge. In four-dimensional space-time the Lagrangian is invariant under superconformal group, i.e., $SO(4, 2)$ discussed above plus translational \mathcal{Q} and superconformal \mathcal{S} transformations^{12,13,14},

$$\delta^{\mathcal{F}} q^a = \frac{i}{2} G_{\mu\nu}^a \sigma_{\mu\nu} \xi - i D^a \gamma_5 \xi, \quad \delta^{\mathcal{F}} B_\mu^a = -i \bar{\xi} \gamma_\mu q^a, \quad \delta^{\mathcal{F}} D^a = \bar{\xi} \mathcal{D}_\mu^{ab} \gamma_\mu \gamma_5 q^a, \quad (27)$$

with non-dynamical auxiliary field D^a and transformation parameter $\xi \equiv \xi_0 - i \not{\xi}_1$. The parameter ξ_0 (ξ_1) parametrizes $\mathcal{F} = \mathcal{Q}$ ($\mathcal{F} = \mathcal{S}$) transformations.

One can construct an $\mathcal{N} = 1$ chiral superfield from certain linear combinations of bosonic, i.e., $\bar{q}q$ and gg , and fermionic, i.e., gq , conformal operators, see Refs.^{15,16}. So that under (27) they transform as Wess-Zumino multiplet. This covariance simplifies the derivation of relations between the anomalies.

We follow the same procedure as in the previous section by using the commutator algebra of the superconformal group for the Green function $\mathcal{G}(z_1, \dots, z_N)$ (20) and use Ward identities to find out consequences. Because of the quantization which require a regularization procedure, the variation of

the action develops an anomaly in d -dimensions for the \mathcal{S} -transformation but not for the \mathcal{Q} -transformation

$$\delta^{\mathcal{Q}}\mathcal{L} = 0, \quad \delta^{\mathcal{S}}\mathcal{L} = \frac{4-d}{2}\bar{\xi}_1 i\sigma_{\mu\nu}G_{\mu\nu}^a q^a. \quad (28)$$

Although there arise contributions in both due to explicit supersymmetry breaking by gauge fixing, however, these sources cannot affect gauge-invariant quantities we deal with. For our purposes we need two commutators from the algebra

$$[\mathcal{Q}, \mathcal{D}]_- = \frac{i}{2}\mathcal{Q}, \quad [\mathcal{Q}, \mathcal{K}_\mu]_- = \gamma_\mu \mathcal{S}. \quad (29)$$

In view of Eq. (28) the first one is non-anomalous and results into a number of relations between the elements of the quark-gluon mixing matrix^{15,16,17}, with the most trivial example involving only the diagonal elements

$${}^{qq}\gamma_j^D + \frac{6}{j} {}^{qq}\gamma_j^D = \frac{j}{6} {}^{qq}\gamma_j^D + {}^{gg}\gamma_j^D. \quad (30)$$

The second commutator in Eq. (29) possesses the superconformal anomaly (28) and, as a result, relations of the type (30), but with γ being replaced by γ^c , are affected in a controllable manner by a computable addendum Δ which arises from renormalization of the operator product¹⁸

$$\mathcal{O}_{jl} i \int d^d z \delta^S \mathcal{L}(z) = \sum_{k=0}^j \Delta_{jk} \mathcal{O}_{k,l-1}. \quad (31)$$

The knowledge of a complete set of such relations allows to compute all entries of the quark-gluon mixing matrix from the knowledge of only one element, e.g., ${}^{qq}\gamma^D + {}^{qq}\gamma^{ND}$. This procedure has successfully been applied in the reconstruction of two-loop off-forward evolution kernels¹⁹.

6 Integrability of three-particle problem

As we explained in the introduction, multi-particle correlations arise as power suppressed effects in hard cross sections and exhibit a genuine quantum mechanical interference of hadron wave functions with different number of constituents. The first non-trivial and the most interesting example is three-particle functions which emerge in hard forward²⁰ and off-forward²¹ Compton scattering in the form of quark-gluon-quark $\langle \bar{q}gq \rangle$ and three-gluon $\langle ggg \rangle$ correlations. Another prominent example is baryon distribution amplitudes⁹. For the sake of definiteness, let us discuss quark-gluon-quark correlators.

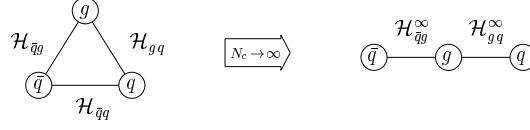


Figure 4. Large- N_c reduction of three-particle $\bar{q}gq$ Hamiltonian.

As all other twist-three sectors, they are distinguished from all even higher-particle sectors by the fact that their basis can be reduced to the one consisting only of quasi-partonic operators¹⁵. This implies that the three-particle kernel of the leading order evolution equation in QCD coupling constant,

$$\frac{d}{d \ln \mu^2} F(\{x\}; \mu^2) = \frac{\alpha_s}{2\pi} \int \prod_i^3 dx_i \delta \left(\sum_j^3 x_j - \eta \right) K(\{x\}; \{x'\}) F(\{x'\}; \mu^2), \quad (32)$$

with $\{x\} = x_1, x_2, x_3$, is merely given by the sum of pair-wise interactions of twist-two kernels discussed in the previous sections, $K = K_{\bar{q}g} + K_{gq} + K_{\bar{q}q}$. As a result of the conformal covariance, established there, the pair-wise kernels in the basis of local conformal operators, to be called \mathcal{H}_{ab} later, depend only on two-particle Casimir operators, $\mathbf{J}_{ab}^2 \equiv J_{ab}(J_{ab} - 1)$, of the conformal group,

$$\mathcal{H} = \mathcal{H}_{\bar{q}g}(J_{\bar{q}g}) + \mathcal{H}_{gq}(J_{gq}) + \mathcal{H}_{\bar{q}q}(J_{\bar{q}q}). \quad (33)$$

The color structure of pair-wise interaction allows to simplify further the diagonalization problem by noticing that $\mathcal{H}_{\bar{q}q}$ vanishes as $1/N_c^2$ relative to $\mathcal{H}_{(\bar{q},q)g}$ in multicolor limit, i.e., $N_c \rightarrow \infty$. Therefore, the three-particle problem on a ring is reduced to the one on a line with the interaction of end sites being neglected, see Fig. 4. Our cherished goal is to solve a Schrödinger equation

$$\mathcal{H}^\infty \Psi \equiv (\mathcal{H}_{\bar{q}g}^\infty + \mathcal{H}_{gq}^\infty) \Psi = N_c \mathcal{E}^\infty \Psi. \quad (34)$$

The explicit form of the pair-wise Hamiltonians depends on the t -channel quantum numbers. For instance, for the operators of the Dirac-color structure $\bar{q}\sigma_{\rho\{\mu} t^c G_{\nu\}\rho}^c q$ they are

$$\frac{1}{N_c} \mathcal{H}_{ab}^\infty(J_{ab}) = \psi(J_{ab} + 3/2) + \psi(J_{ab} - 3/2) - 2\psi(1), \quad (35)$$

where $\psi(x) = d \ln \Gamma(x)/dx$ and the indices run over $a = (\bar{q}, q)$ and $b = g$. The large- N_c Hamiltonian \mathcal{H}^∞ describes a three-site inhomogeneous integrable open spin chain model. Integrability means that it possesses a complete set of integrals of motion matching the number of degrees of freedom. The problem

admits a representation in terms of the \mathcal{R} -matrix acting on a tensor product of vector spaces $V_a \otimes V_b$ and satisfying Yang-Baxter relation ²²,

$$\mathcal{R}_{ab}(\lambda) \equiv \begin{array}{c} a \\ | \\ \hline | \\ b \end{array}, \quad \begin{array}{c} c \\ \diagup \quad \diagdown \\ a \quad b \\ \diagdown \quad \diagup \\ c \end{array} = \begin{array}{c} a \\ \diagdown \quad \diagup \\ b \quad c \\ \diagup \quad \diagdown \\ a \end{array} \quad (36)$$

One of the solutions to the Yang-Baxter equation is given by $\mathcal{R}_{ab}(\lambda) \sim \Gamma(J_{ab} + \lambda)/\Gamma(J_{ab} - \lambda)$. The construction by Sklyanin ²³ allows to find the Hamiltonian corresponding to this \mathcal{R} -matrix via the following graphic equation ^{24,25}

$$\mathcal{H}^\infty = \frac{1}{2} \frac{d}{d\lambda} \Big|_{\lambda=0} \ln \left\{ \begin{array}{c} q \quad g \quad \bar{q} \\ | \quad | \quad | \\ \hline | \quad | \quad | \\ g \quad g \quad g \\ | \quad | \quad | \\ 1 \end{array} \right\}. \quad (37)$$

The spectral parameter λ in the q and \bar{q} sites is shifted as $\lambda \pm 3/2$. The picture is self explanatory: the three \mathcal{R} -matrices with dimensions of spaces as displayed are aligned next to each other, then reflected with the unity matrix and traced in the auxiliary space with their inverse. The resulting object is called the transfer matrix. Its logarithmic derivative determines the qgq Hamiltonian up to an additive constant.

The Yang-Baxter equation holds for an arbitrary dimension of the vector spaces. When the auxiliary space is two-dimensional, one finds another solution to (36), $\mathcal{R}_{a,1/2}(\lambda) = \lambda 1 + \sigma^i J_a^i$. Calculating the transfer matrix for the two-dimensional auxiliary space, one identifies two operators ^{26,24,25}

$$\mathbf{J}^2 = \mathbf{J}_{qg}^2 + \mathbf{J}_{q\bar{q}}^2 + \mathbf{J}_{\bar{q}g}^2, \quad \mathbf{Q} = [\mathbf{J}_{qg}^2, \mathbf{J}_{\bar{q}g}^2]_+ - 2(3/2)^2 (\mathbf{J}_{qg}^2 + \mathbf{J}_{\bar{q}g}^2), \quad (38)$$

which commute with the Hamiltonian (37) by construction since all of them are deduced from bundles satisfying the Yang-Baxter equation.

Thus instead of diagonalizing the Hamiltonian one can attempt to solve a much simple eigenvalue problem for the fourth-order differential operator \mathbf{Q} . Because of commutativity, the Hamiltonian shares the same eigenfunctions Ψ . Thus the eigenvalues \mathcal{E}^∞ of \mathcal{H}^∞ are functions of quantized values J and Q of the integrals of motion \mathbf{J}^2 and \mathbf{Q} . The problem was solved using WKB, i.e., large- J , approximation with the result for energy levels ^{26,24,25}

$$\mathcal{E}_0^\infty(J) = \psi(J+3) + \psi(J+4) - 2\psi(1) - 1/2, \quad (39)$$

$$\mathcal{E}^\infty(J, Q) = 2 \ln J + 2 \operatorname{Re} \psi \left(3/2 + i \sqrt{(2Q/J^2 - 3)/4} \right) - 4\psi(1) - 3/2,$$

where the special value \mathcal{E}_0^∞ is separated from the rest of the spectrum by a gap and was known for some time ²⁷. Full account of this and other exactly solvable cases can be found in the literature ^{24,25,28}.

We would like to thank the organizers of the workshop for such an interesting meeting and INT (Seattle) for support. This work was supported by the US Department of Energy under contract DE-FG02-93ER40762.

References

1. G. Sterman, Int. J. Mod. Phys. A 16 (2001) 3041.
2. see, e.g., the contribution by Yu.V. Kovchegov, hep-ph/0202238.
3. S. Chekanov et al., Eur. Phys. J. C 21 (2001) 443.
4. X. Ji, J. Phys. G 24 (1998) 1181.
5. A.V. Radyushkin, hep-ph/0101225.
6. K. Goeke, M.V. Polyakov, M. Vanderhaeghen, Prog. Part. Nucl. Phys. 47 (2001) 401.
7. A.V. Belitsky, D. Müller, A. Kirchner, hep-ph/0112108.
8. G. Mack, A. Salam, Ann. Phys. 53 (1969) 174.
9. S.J. Brodsky, G.P. Lepage, Phys. Rev. D 22 (1980) 2157.
10. A.V. Efremov, A.V. Radyushkin, Phys. Lett. B 94 (1980) 245.
11. A.V. Belitsky, D. Müller, Phys. Lett. B 417 (1998) 129; Nucl. Phys. B 527 (1998) 207; Nucl. Phys. B 537 (1999) 397.
12. J. Wess, B. Zumino, Nucl. Phys. B 70 (1974) 39.
13. S. Ferrara, Nucl. Phys. B 77 (1974) 73.
14. P.H. Dondi, M.F. Sohnius, Nucl. Phys. B 81 (1974) 317.
15. A.P. Bukhvostov, G.V. Frolov, L.N. Lipatov, E.A. Kuraev, Nucl. Phys. B 258 (1985) 601.
16. A.V. Belitsky, D. Müller, A. Schäfer, Phys. Lett. B 450 (1999) 126.
17. A.V. Belitsky, D. Müller, Nucl. Phys. B (Proc. Suppl.) 79 (1999) 576.
18. A.V. Belitsky, D. Müller, Phys. Rev. D 65 (2002) 054037.
19. A.V. Belitsky, D. Müller, A. Freund, Nucl. Phys. B 574 (2000) 347.
20. R.L. Jaffe, X. Ji, Nucl. Phys. B 375 (1992) 527.
21. A.V. Belitsky, D. Müller, Nucl. Phys. B 589 (2000) 611.
22. L.D. Faddeev, hep-th/9605187.
23. E.K. Sklyanin, J. Phys. A 21 (1988) 2375.
24. A.V. Belitsky, Phys. Lett. B 453 (1999) 59; Nucl. Phys. B 558 (1999) 259; Nucl. Phys. B 574 (2000) 407.
25. S.E. Derkachov, G.P. Korchemsky, A.N. Manashov, Nucl. Phys. B 566 (2000) 203.
26. V.M. Braun, S.E. Derkachov, A.N. Manashov, Phys. Rev. Lett. 81 (1998) 2020.
27. I.I. Balitsky, V.M. Braun, Y. Koike, K. Tanaka, Phys. Rev. Lett. 77 (1996) 3078.
28. V.M. Braun, S.E. Derkachov, G.P. Korchemsky, A.N. Manashov, Nucl. Phys. B 553 (1999) 355.